


RESEARCH

Open Access



# The role of myeloid cell heterogeneity during spontaneous choroidal neovascularization in *Vldlr* knockout mice

Amrita Rajesh<sup>1</sup>, Joyce Gong<sup>1</sup>, Kyle S Chan<sup>1</sup>, Ritvik Viniak<sup>1</sup>, Steven Droho<sup>1</sup>, David Kachar<sup>1</sup>, Joshua Y Strauss<sup>1</sup>, Andrew L. Wang<sup>1</sup> and Jeremy A. Lavine<sup>1\*</sup> 

## Abstract

**Background** Myeloid cells are heterogeneous cells that are critical for spontaneous choroidal neovascularization (CNV) in the *Vldlr*<sup>-/-</sup> mouse model. However, the specific myeloid cell subtype necessary for CNV remains unknown.

**Methods and results** To investigate the role of monocytes, we bred *Ccr2*<sup>-/-</sup> and *Nr4a1*<sup>-/-</sup> mice into the *Vldlr*<sup>-/-</sup> background. We found that *Ccr2* and *Nr4a1* deficiency had no effect upon macrophage counts, CNV lesion number, or total CNV area. Next, we investigated the role of microglia by generating *Vldlr*<sup>-/-</sup>*Tmem119*<sup>CreER/+</sup>*Rosa26*<sup>DTR/+</sup> mice. Diphtheria toxin (DT) treatment reduced macrophage counts at CNV lesions and CNV lesion number, but did not affect total CNV lesion area. To target microglia via a second strategy, we generated *Vldlr*<sup>-/-</sup>*Cx3cr1*<sup>CreER</sup>*Csf1r*<sup>iDTR</sup> mice and treated them with a single low dose of tamoxifen to target microglia without affecting choroidal macrophages. DT treatment in *Vldlr*<sup>-/-</sup>*Cx3cr1*<sup>CreER</sup>*Csf1r*<sup>iDTR</sup> mice decreased macrophage counts at CNV lesions and CNV lesion number but again had no effect upon total CNV lesion area. To target choroidal macrophages and microglia, we treated *Vldlr*<sup>-/-</sup>*Cx3cr1*<sup>CreER</sup>*Csf1r*<sup>iDTR</sup> mice with 9 tamoxifen treatments. DT-treated mice showed dramatic reductions in macrophage counts, CNV number, and total lesion area.

**Conclusions** These data suggest that monocytes and monocyte-derived macrophages are dispensable, microglia are likely initiators for CNV development, and choroidal macrophages are potential key contributors to CNV growth and/or maintenance in the *Vldlr*<sup>-/-</sup> model.

**Keywords** Angiogenesis, Choroidal neovascularization, Macrophage, Macular degeneration, Microglia, *Vldlr*

\*Correspondence:

Jeremy A. Lavine  
jeremy.lavine@northwestern.edu

<sup>1</sup>Department of Ophthalmology, Feinberg School of Medicine,  
Northwestern University, 240. E. Huron St., McGaw M343, Chicago,  
IL 60614, USA



© The Author(s) 2025. **Open Access** This article is licensed under a Creative Commons Attribution-NonCommercial-NoDerivatives 4.0 International License, which permits any non-commercial use, sharing, distribution and reproduction in any medium or format, as long as you give appropriate credit to the original author(s) and the source, provide a link to the Creative Commons licence, and indicate if you modified the licensed material. You do not have permission under this licence to share adapted material derived from this article or parts of it. The images or other third party material in this article are included in the article's Creative Commons licence, unless indicated otherwise in a credit line to the material. If material is not included in the article's Creative Commons licence and your intended use is not permitted by statutory regulation or exceeds the permitted use, you will need to obtain permission directly from the copyright holder. To view a copy of this licence, visit <http://creativecommons.org/licenses/by-nc-nd/4.0/>.

## Background

Age-related macular degeneration (AMD) is a leading cause of blindness in the developed world. Vision loss from AMD occurs from either photoreceptor atrophy (geographic atrophy) in advanced dry AMD [1], or destructive angiogenesis into the retina (termed choroidal neovascularization [CNV]) in neovascular AMD [2]. Neovascular AMD is treated with frequent intravitreal anti-vascular endothelial growth factor (VEGF) injections, but up to 33% of patients do not experience visual acuity improvement [3]. Recent advances include longer-lasting anti-VEGF formulations [4, 5]; however, treatment resistance remains a significant problem for neovascular AMD patients.

Neovascular AMD is modeled by both the laser-induced CNV mouse model and spontaneous CNV models, such as the *Vldlr*<sup>-/-</sup> mouse. The *Vldlr*<sup>-/-</sup> mouse differs from the laser-induced CNV model because connections develop between retinal and choroidal neovascularization in the subretinal space, most mimicking the type 3 CNV in patients, which is present in both neovascular AMD and type 2 macular telangiectasia [6]. Spontaneous CNV develops due to an absence of very-low-density lipoprotein receptor (VLDLR) expression in photoreceptors, impairing their ability to uptake triglyceride as an energy source [7]. When lipid uptake into photoreceptors is disrupted and plasma lipid levels are elevated, glucose transport is paradoxically reduced. This results in fatty acid- and glucose-starved photoreceptors, which stabilizes hypoxia-induced factor 1 and increases VEGF expression, leading to spontaneous CNV [7]. Similar to studies in the laser-induced CNV model, pharmacologic or genetic ablation of all macrophages in *Vldlr*<sup>-/-</sup> mice using colony stimulating factor 1 receptor (CSF1R) antagonists or *Cx3cr1*<sup>CreER</sup>*Rosa26*<sup>DTR</sup> mice reduces spontaneous CNV [8]. Given the new tools that are now available to specifically target different ocular myeloid cell populations, it is imperative to identify the specific myeloid populations that drive CNV in the *Vldlr*<sup>-/-</sup> mouse model.

Macrophages express multiple complement components and receptors, which are extensively linked to AMD in genome wide association studies [9, 10, 11, 12]. Furthermore, macrophages are detectable in human excised CNV membranes [13, 14], and are necessary for the laser-induced CNV mouse model [15, 16]. Potential myeloid cell contributors to CNV include yolk-sac derived microglia, monocyte-derived choroidal macrophages, and extravasated classical and non-classical monocytes [17, 18]. Microglia exist in the plexiform layers of the retina, are derived from yolk sac progenitors, and could regulate CNV in *Vldlr*<sup>-/-</sup> mice by migrating posteriorly to the CNV lesions. Microglia can now be targeted with new state-of-the-art models including

*P2ry12*<sup>CreER</sup> and *Tmem119*<sup>CreER</sup> mice, which specifically target microglia compared to other macrophages [19, 20, 21, 22]. Prior studies in *Vldlr*<sup>-/-</sup> mice are yet to use these newer models to specifically target microglia; thus, their specific role is not entirely elucidated. Choroidal macrophages are derived from blood monocytes [17] and could migrate anteriorly from the choroid into the CNV lesions in *Vldlr*<sup>-/-</sup> mice, but are otherwise poorly studied and no specific markers for choroidal macrophages exist. In both the laser-induced CNV and *Vldlr*<sup>-/-</sup> models, no studies have specifically investigated the role of choroidal macrophages. Non-classical monocytes are derived from classical monocytes via the key transcription factor NR4A1 [23]. Non-classical monocytes can migrate into tissue and differentiate into non-classical monocyte-derived macrophages at CNV lesions. Using *Nr4a1*<sup>-/-</sup> mice, which are deficient in non-classical monocytes, our group has shown that non-classical monocytes are dispensable during laser-induced CNV [24]. However, the role of non-classical monocytes during CNV in *Vldlr*<sup>-/-</sup> mice remains unknown. Finally, classical monocytes can extravasate from the blood and differentiate into classical monocyte-derived macrophages at CNV lesions. In the laser-induced CNV model, our group and others have shown that monocyte-derived macrophages from extravasated classical monocytes are necessary for CNV [25, 26, 27], using *Ccr2*<sup>-/-</sup> mice, which are a mouse model where classical monocytes are present but are deficient in their ability to emigrate from the bone marrow to blood and the blood to tissue [28]. Furthermore, using single-cell RNA-sequencing, we have shown that a subset of classical monocyte-derived macrophages which express *Spp1* and CD11c markers drive angiogenesis through multimodal pro-angiogenic pathways [24, 29]. Despite these advances in the laser-induced CNV model, the laser model stimulates an acute inflammatory reaction that poorly models chronic inflammation in AMD. Therefore, the goal of this study was to investigate the role of each myeloid cell type in the *Vldlr*<sup>-/-</sup> mouse.

First, we recapitulated prior results and showed that CSF1R pharmacologic inhibition reduced macrophage numbers at CNV lesions and are necessary for CNV lesions in *Vldlr*<sup>-/-</sup> mice. Next, we bred *Ccr2*<sup>-/-</sup> and *Nr4a1*<sup>-/-</sup> mice into the *Vldlr*<sup>-/-</sup> mouse background. In *Ccr2*<sup>-/-</sup> mice, classical monocytes lack the ability to extravasate from bone marrow and blood. Alternatively, *Nr4a1*<sup>-/-</sup> mice lack a key transcription factor for non-classical monocyte development from classical monocytes [23]. Thus, *Vldlr*<sup>-/-</sup>*Ccr2*<sup>-/-</sup> and *Vldlr*<sup>-/-</sup>*Nr4a1*<sup>-/-</sup> mice will investigate the role of classical and non-classical monocyte-derived macrophages in *Vldlr*<sup>-/-</sup> mice, respectively. We investigated microglia with two complementary approaches: *Vldlr*<sup>-/-</sup>*Tmem119*<sup>CreER</sup>*Rosa*<sup>DTR</sup> and *Vldlr*<sup>-/-</sup>*Cx3cr1*<sup>CreER</sup>*Csf1*<sup>iDTR</sup> mice.

*Vldlr*<sup>-/-</sup>*Tmem119*<sup>CreER</sup>*Rosa*<sup>DTR</sup> mice were given 9 tamoxifen injections over 3 weeks to maximize microglia targeting before diphtheria toxin (DT) treatment to deplete microglia. *Vldlr*<sup>-/-</sup>*Cx3cr1*<sup>CreER</sup>*Csf1r*<sup>iDTR</sup> mice received a single tamoxifen injection followed by a 2 week wash out period prior to DT treatment to specifically target microglia without affecting choroidal macrophages. Finally, *Vldlr*<sup>-/-</sup>*Cx3cr1*<sup>CreER</sup>*Csf1r*<sup>iDTR</sup> mice were administered 9 tamoxifen injections to simultaneously target microglia and choroidal macrophages before DT-based ablation. We found that classical and non-classical monocytes were not necessary for spontaneous CNV. In microglia-depleted mice, CNV lesion number was reduced but total CNV lesion area was unchanged. In microglia and choroidal macrophage ablated mice, CNV lesion number and total CNV lesion area were severely reduced. These data suggest that microglia may be CNV initiators, and choroidal macrophages are potential contributors to CNV growth and/or maintenance in *Vldlr*<sup>-/-</sup> mice.

## Methods

### Sex as a biological variable

All studies were carried out on mixed sex populations with a minimum of 8 animals per sex per group. All data were investigated for sex-specific effects, and none were found.

### Animals

Wildtype C57BL/6J (#000664), *Vldlr*<sup>-/-</sup> (#002529), *Ccr2*<sup>-/-</sup> (#004999), *Nr4a1*<sup>-/-</sup> (#006187), *Tmem119*<sup>CreER</sup> (#031820), *Cx3cr1*<sup>CreER</sup> (#020940), *Rosa26*<sup>CAG-LSL-DTR</sup> (#007900), and *Csf1r*<sup>CAG-LSL-DTR</sup> (#0124046) mice were purchased from Jackson Labs (Bar Harbor, ME). Wildtype C57BL/6J and *Vldlr*<sup>-/-</sup> mice were bred and maintained within a pathogen-free barrier environment at the Center for Comparative Medicine at Northwestern University. Mice were bred as outlined in the results. Because *Vldlr*<sup>-/-</sup> mice are on a mixed background, all experiments were performed compared to littermate controls. Genotyping was performed by Transnetyx (Cordova, TN) to confirm the absence of the RD8 allele (*Crb1*<sup>-</sup>). All studies adhered to the ARVO Statement for Animal Use in Ophthalmic and Vision Research and received approval from the Northwestern University Institutional Animal Care and Use Committee. All experiments were carried out on 6–7 week-old mice.

### CSF1R antagonist administration

Ki 20,227 (44-815-0) was purchased from Tocris Biosciences (Bristol, UK), and dissolved in DMSO. At 6 weeks of age, mice were treated with 4 consecutive intraperitoneal injections of DMSO or Ki 20,227 (50 mg/kg).

Animals were euthanized on Day 5 for retinal and choroidal wholemount immunofluorescence imaging.

### Tamoxifen administration

Tamoxifen (#T5648, Millipore Sigma, Burlington, MA) was dissolved overnight at 37°C in corn oil at 20 mg/ml or 40 mg/ml. A single intraperitoneal injection of tamoxifen (20 mg/ml, 100 mg/kg) was given to *Cx3cr1*<sup>CreER</sup>*Csf1r*<sup>iDTR</sup> or *Vldlr*<sup>-/-</sup>*Cx3cr1*<sup>CreER</sup>*Csf1r*<sup>iDTR</sup> mice at Week 4 of age to target microglia. Nine intraperitoneal injections of tamoxifen (20 mg/ml, 100 mg/kg) were given 3 times per week to *Cx3cr1*<sup>CreER</sup>*Csf1r*<sup>iDTR</sup> or *Vldlr*<sup>-/-</sup>*Cx3cr1*<sup>CreER</sup>*Csf1r*<sup>iDTR</sup> mice from Week 3 to Week 6 to target microglia and choroidal macrophages. Nine intraperitoneal injections of tamoxifen (40 mg/ml, 200 mg/kg) were given 3 times per week to *Tmem119*<sup>CreER/+</sup>*Rosa*<sup>DTR/+</sup> or *Vldlr*<sup>-/-</sup>*Tmem119*<sup>CreER/+</sup>*Rosa*<sup>DTR/+</sup> mice from Week 3 to Week 6 to target microglia.

### Diphtheria toxin administration

At 6 weeks of age, intraperitoneal injections of sterile PBS vehicle control or 100ng of DT (#322326, Millipore Sigma) in 0.1 mL of PBS were administered for 4 consecutive days to *Cx3cr1*<sup>CreER</sup>*Csf1r*<sup>iDTR</sup> or *Vldlr*<sup>-/-</sup>*Cx3cr1*<sup>CreER</sup>*Csf1r*<sup>iDTR</sup> mice to target microglia. Intraperitoneal injections of PBS or 500ng DT were administered for 4 consecutive days to *Tmem119*<sup>CreER/+</sup>*Rosa*<sup>DTR/+</sup> or *Vldlr*<sup>-/-</sup>*Tmem119*<sup>CreER/+</sup>*Rosa*<sup>DTR/+</sup> mice to target microglia and *Cx3cr1*<sup>CreER</sup>*Csf1r*<sup>iDTR</sup> or *Vldlr*<sup>-/-</sup>*Cx3cr1*<sup>CreER</sup>*Csf1r*<sup>iDTR</sup> mice to target microglia and choroidal macrophages. Mice were sacrificed on Day 5 for immunofluorescence imaging.

### Immunofluorescence imaging of retinal flatmounts

Confocal microscopy was performed as previously described [30]. Briefly, mice were euthanized, eyes were enucleated, and retinas were isolated then fixed in 4% paraformaldehyde (#15713-S; Electron Microscopy Sciences, Hatfield, PA, USA) for 1 h at room temperature. Retinas were blocked in blocking buffer including TBS + 5% Donkey Serum (#S30, Sigma-Aldrich, St. Louis, MO) + 2.5% bovine serum albumin (A2153, Sigma) + 0.5% Triton X-100 (X100; Sigma) overnight at 4°C. Primary incubations were next performed overnight at 4°C (Table S1). Retinas were washed 5 times in TBS-T (TBS with 0.5% Tween-20, #00777; Amresco, Solon, OH, USA), and secondary antibody incubations were performed overnight at 4°C (Table S1). Retinas were washed again with TBS-T five times and mounted on HistoBond microscope slides (#16004–406, VWR; Batavia, IL, USA) with Immu-Mount (#9990402; ThermoFisher, Carlsbad, CA, USA). Nikon W1 Dual CAM Spinning Disk Microscope was used with Nikon NIS Elements software for imaging. Images were masked and quantitated in FIJI using

the Cell Counter to generate macrophage and microglia density.

#### Immunofluorescence imaging of *Vldlr*<sup>-/-</sup> choroidal flatmounts

Mice were euthanized, eyes were enucleated and immediately fixed in 4% paraformaldehyde for 1 h at room temperature. Next, choroidal flatmounts were dissected and blocked overnight at 4°C. Primary antibody incubations were also performed overnight at 4°C (Table S1). Choroids were washed 5 times in TBS-T, incubated overnight in secondary antibody, washed 5 times in TBS-T, and mounted as described above. Nikon W1 Dual CAM Spinning Disk Microscope was used with Nikon NIS Elements software for imaging. Images were masked. CNV number and area was quantitated in FIJI using the ROI manager tool. Macrophage numbers were quantitated by Thresholding the IBA1 channel, deleting the optic nerve, and using the analyze particles to count any cell >20 microns in area.

#### Immunofluorescence imaging of choroidal flatmounts

Mice were euthanized, eyes were enucleated, and choroidal wholemounts were dissected. Choroidal flatmounts were fixed in 4% paraformaldehyde for 1 h at room temperature and blocked as described above overnight at 4°C. Next, choroids were incubated with primary antibodies overnight at 4°C (Table S1). Choroids were washed twice in TBS-T, fixed for 1 h with 4% paraformaldehyde at room temperature, washed twice in TBS-T, and bleached 1% hydrogen peroxide (#BP2633500, ThermoFisher) diluted in PBS. Bleaching was performed for 45 min at 55°C, repeated five times as previously described [31]. Choroids were washed three times in TBS-T and blocked in blocking solution for 30 min at room temperature. Secondary antibodies incubations were performed overnight at 4°C, washed five times in TBS-T, and mounted. Nikon W1 Dual CAM Spinning Disk Microscope was used with Nikon NIS Elements software for imaging. Images were masked and quantitated in FIJI using the Cell Counter to generate choroidal macrophage density.

#### Statistical analysis

Data were assessed for normality using the Shapiro-Wilk test. Comparisons between two groups were made using Mann-Whitney test if not normally distributed or either Student's unpaired t-test or Welch's t-test if data were normally distributed, depending upon if the standard deviations were different. If more than 3 groups were compared, data were compared using One-Way ANOVA or Brown-Forsythe and Welch ANOVA. See figure legends for the exact test used for each comparison. A

p-value < 0.05 was considered statistically significant. All data are presented as mean ± standard error mean.

#### Results

To corroborate prior reports that macrophages are necessary for spontaneous CNV in *Vldlr*<sup>-/-</sup> mice [8], 6-week-old male and female mice were treated with CSF1R antagonist for 4 consecutive days by intraperitoneal injection (Fig. 1A). Because *Vldlr*<sup>-/-</sup> mice are on a mixed background, all experiments were performed and compared to littermate controls. On Day 5, mice were sacrificed, eyes were enucleated, and choroidal wholemounts were processed for immunofluorescence imaging. Representative choroidal wholemount images are shown in Fig. 1B–C. To assess the effectiveness of the CSF1R antagonist ablation of macrophages at CNV lesions, we counted IBA1<sup>+</sup> cells (a pan-macrophage marker) in Podocalyxin<sup>+</sup> (a choroidal capillary marker) CNV lesions on choroidal wholemounts. Podocalyxin<sup>+</sup> CNV lesions are easily detectable and not masked by healthy retinal pigment epithelium (RPE), which blocks underlying choroidal capillaries from being visualized. CSF1R inhibition reduced IBA1<sup>+</sup> cells at CNV lesions by 63% ( $p < 0.0001$ , Fig. 1D). Furthermore, CNV lesion number was decreased by 28% ( $p < 0.05$ , Fig. 1E), and CNV lesion area reduced by 48% ( $p < 0.0001$ , Fig. 1F). Data split by sex can be found in Fig S1. These data at 6 weeks of age agree with prior findings at 2–4 weeks of age [8]. As discussed in the introduction, IBA1<sup>+</sup> cells in CNV lesions could be microglia, choroidal macrophages, or monocyte-derived macrophages. In the presence of the disease model, it is very challenging to determine the origin of the IBA1<sup>+</sup> cells at the lesion because the cells may adopt different markers in a new microenvironment. Therefore, we next assessed the effectiveness of the CSF1R antagonist in wildtype mice to determine if microglia and/or choroidal macrophages can be target by CSF1R antagonism for depletion (Fig S2A). Four days of CSF1R inhibition decreased retinal microglia in the outer plexiform layer / deep capillary plexus by 84% ( $p < 0.0001$ , Fig S2B–D). Similarly, choroidal macrophage density was reduced by 90% ( $p < 0.0001$ , Fig S2E–G). These data suggest that CSF1R antagonism could be inhibiting CNV by ablating microglia, choroidal macrophages, and/or monocyte-derived macrophages that also depend upon CSF1R signaling.

Since the laser-induced CNV model is dependent upon classical monocyte-derived macrophages [25, 26, 27], we crossed the classical monocyte defective *Ccr2*<sup>-/-</sup> mouse into the *Vldlr*<sup>-/-</sup> mixed strain background. We bred *Vldlr*<sup>-/-</sup>*Ccr2*<sup>+/-</sup> mice to generate littermate control *Vldlr*<sup>-/-</sup>*Ccr2*<sup>+/+</sup> mice, *Vldlr*<sup>-/-</sup>*Ccr2*<sup>+/-</sup> mice, and *Vldlr*<sup>-/-</sup>*Ccr2*<sup>-/-</sup> mice, which were born in appropriate mendelian ratios (Fig. 2A). *Vldlr*<sup>-/-</sup>*Ccr2*<sup>-/-</sup> mice are



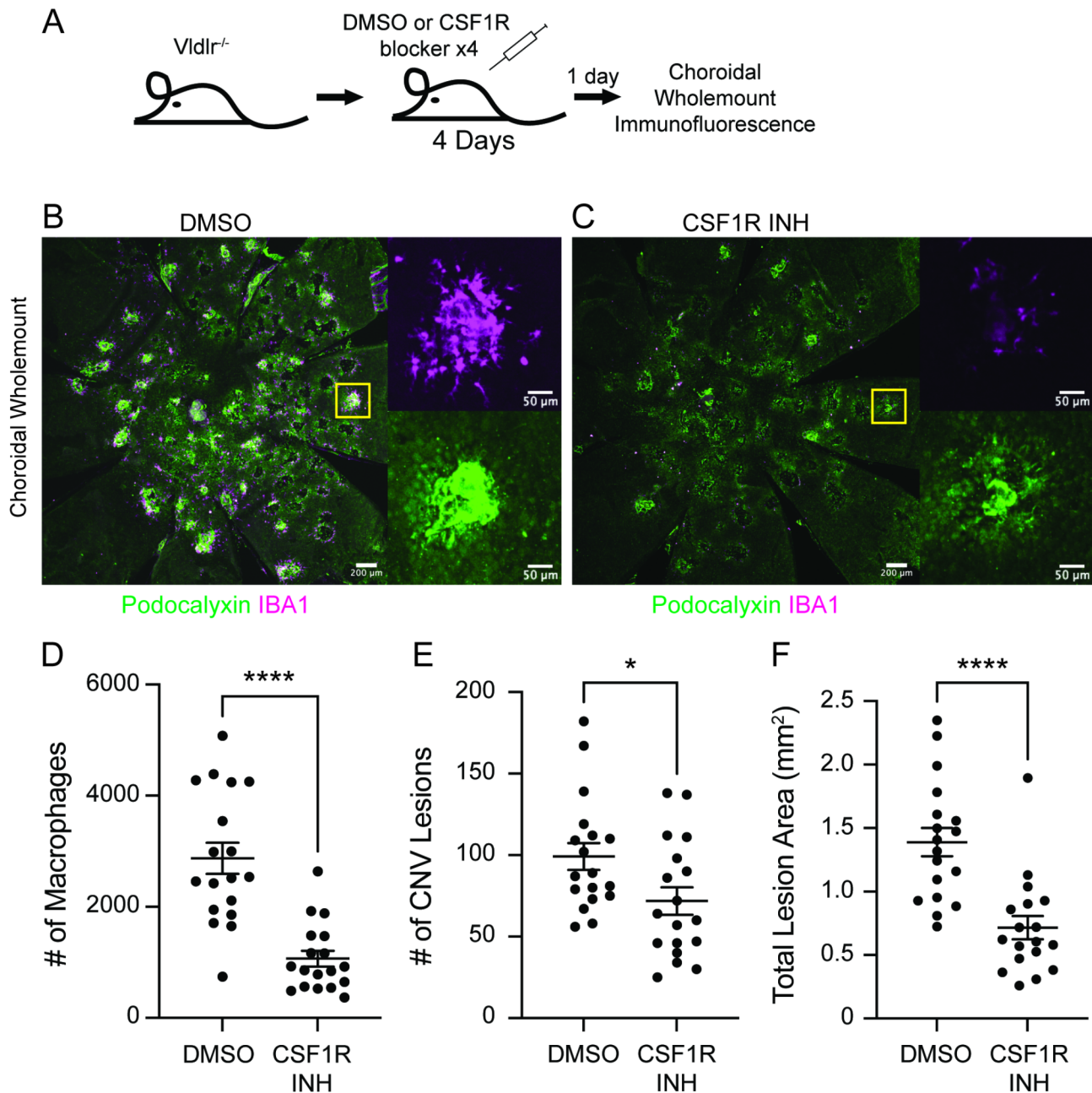


**Fig. 1** Ocular macrophages are necessary for CNV in *Vldlr*<sup>-/-</sup> mice. **A:** Schematic for injection strategy in *Vldlr*<sup>-/-</sup> mice. **B-C:** Representative choroidal wholemount images of DMSO vehicle control and CSF1R inhibitor (INH) treated mice stained for IBA1 (macrophages) and Podocalyxin (choriocapillaris). Insets are outlined in yellow. CSF1R inhibition reduced macrophage counts (**D**, Mann-Whitney test), the number of CNV lesions (**E**, Student's unpaired t-test), and total CNV lesion area (**F**, Student's unpaired t-test). \*  $p < 0.05$ , \*\*\*\*  $p < 0.0001$ .  $N = 18$  mice per group

deficient in classical monocytes and classical monocyte-derived macrophages. Representative choroidal wholemounts of 6-week-old mice are shown in Fig. 2B-D. We found that the *Ccr2*<sup>-/-</sup> allele had no effect upon lesion number, CNV area, or macrophage counts at CNV lesions (Fig. 2E-G). These data suggest, in contrast to the laser-induced CNV model, that classical monocytes and classical monocyte-derived macrophages are dispensable in the spontaneous *Vldlr*<sup>-/-</sup> CNV model.

Next, we bred the non-classical monocyte deficient *Nr4a1*<sup>-/-</sup> mouse into the *Vldlr*<sup>-/-</sup> mixed strain background to investigate the role of non-classical monocytes. We crossed *Vldlr*<sup>-/-</sup>*Nr4a1*<sup>+/-</sup> mice to create littermate control *Vldlr*<sup>-/-</sup>*Nr4a1*<sup>+/+</sup> mice, *Vldlr*<sup>-/-</sup>*Nr4a1*<sup>+/-</sup> mice, and *Vldlr*<sup>-/-</sup>*Nr4a1*<sup>-/-</sup> mice, which were also born in expected mendelian ratios (Fig. 3A). *Vldlr*<sup>-/-</sup>*Nr4a1*<sup>-/-</sup> mice are deficient in non-classical monocytes and non-classical monocyte-derived macrophages. Eyes were

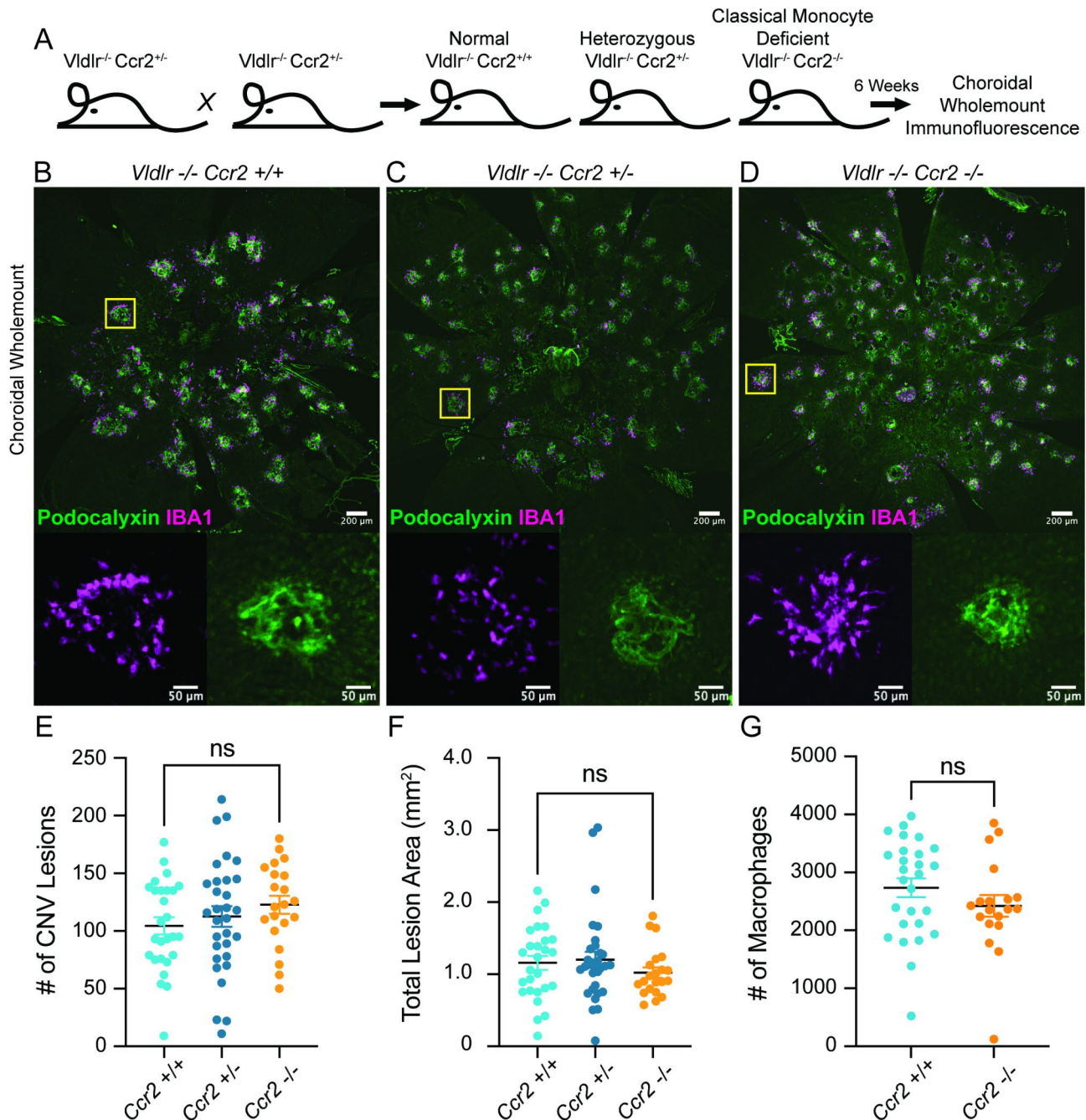


**Fig. 2** Classical monocyte-derived macrophages are dispensable for CNV in *Vldlr*<sup>-/-</sup> mice. **A:** Schematic for breeding injection strategy in *Vldlr*<sup>-/-</sup> mice. **B–D:** Representative choroidal wholemount images of *Ccr2*<sup>+/+</sup>, *Ccr2*<sup>+/-</sup>, and *Ccr2*<sup>-/-</sup> mice stained for IBA1 (macrophages) and Podocalyxin (choriocalpillaris). Insets are outlined in yellow. The number of CNV lesions (**E**, One-Way ANOVA, *N* = 21–31 per group), total CNV lesion area (**F**, Brown-Forsythe and Welch ANOVA, *N* = 21–31 per group), and macrophage counts (**G**, Mann-Whitney test, *N* = 19–27 per group) were equal between groups. ns = not significant

harvested at 6 weeks of age and representative choroidal wholemounts are shown in Fig. 3B–D. *Vldlr*<sup>-/-</sup> *Nr4a1*<sup>+/+</sup> mice, *Vldlr*<sup>-/-</sup> *Nr4a1*<sup>+/-</sup> mice, and *Vldlr*<sup>-/-</sup> *Nr4a1*<sup>-/-</sup> mice demonstrated comparable lesion number, CNV area, and macrophage counts in CNV lesions (Fig. 3E–G). These data suggest, in agreement with the laser-induced CNV model [24], that non-classical monocytes and

non-classical monocyte-derived macrophages are dispensable in the spontaneous *Vldlr*<sup>-/-</sup> CNV model. These data agree with prior work that monocytes are absent from CNV lesions in *Vldlr*<sup>-/-</sup> mice [32].

Since classical and non-classical monocytes are not necessary for CNV in *Vldlr*<sup>-/-</sup> mice, we next sought to investigate retinal microglia and choroidal macrophages.



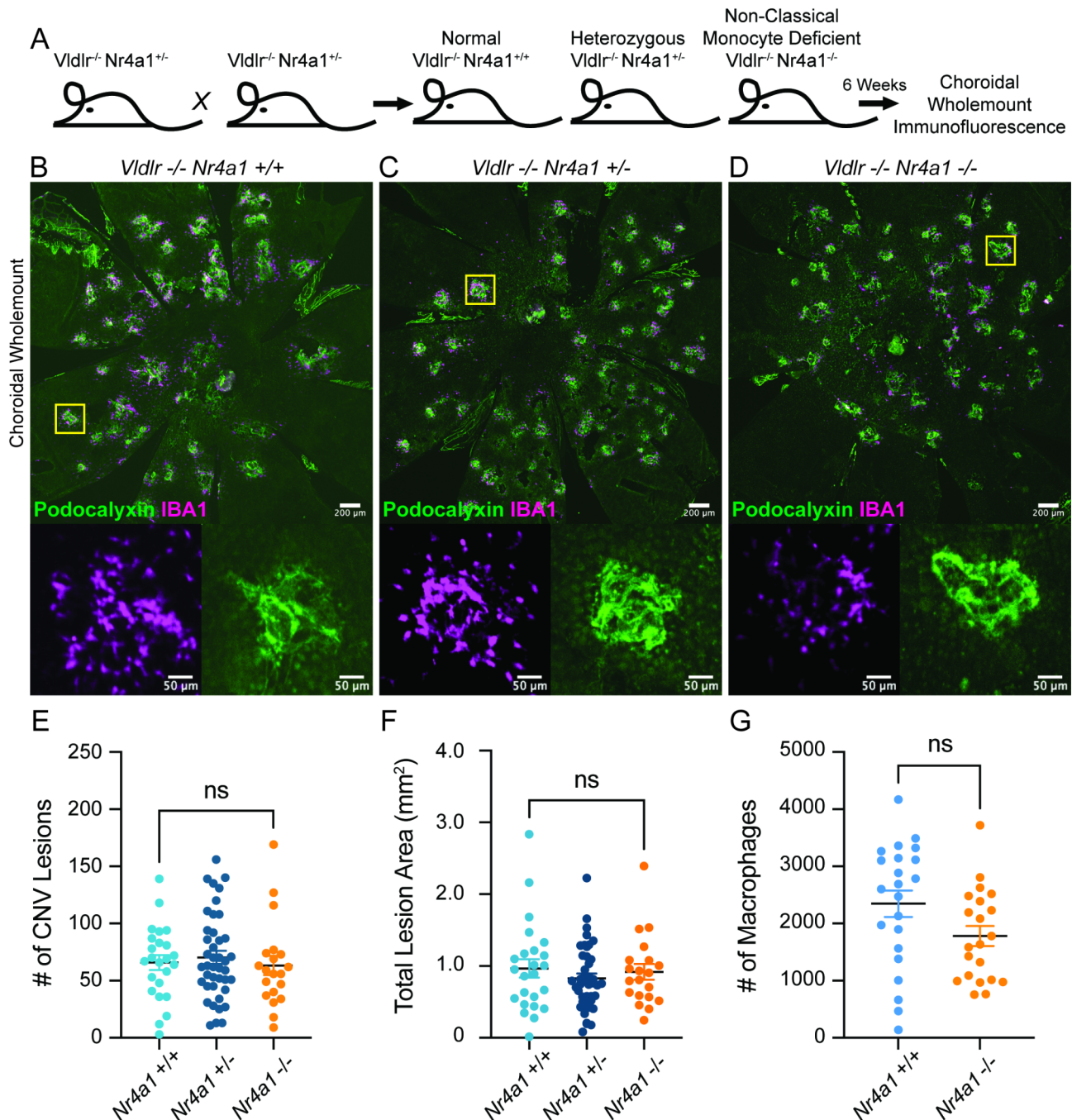


**Fig. 3** Non-classical monocyte-derived macrophages are not necessary for CNV in *Vldlr*<sup>-/-</sup> mice. **A:** Schematic for breeding injection strategy in *Vldlr*<sup>-/-</sup> mice. **B–D:** Representative choroidal wholemount images of *Nr4a1*<sup>+/+</sup>, *Nr4a1*<sup>+/-</sup>, and *Nr4a1*<sup>-/-</sup> mice stained for IBA1 (macrophages) and Podocalyxin (choriocapillaris). Insets are outlined in yellow. The number of CNV lesions (**E**, One-Way ANOVA, *N*=20–42 per group), total CNV lesion area (**F**, One-Way ANOVA, *N*=20–42 per group), and macrophage counts (**G**, Student's unpaired t-test, *N*=21–22 per group) were equal between groups. ns=not significant

We first targeted yolk-sac derived retina microglia via *Tmem119*<sup>CreER</sup> mice, which specifically target microglia over other macrophage populations [19, 20, 22]. We bred *Tmem119*<sup>CreER</sup> and *Rosa*<sup>DTR</sup> mice. In this mouse model, tamoxifen will induce CRE expression in microglia, resulting in the expression of the diphtheria toxin

receptor (DTR), making microglia susceptible to DT-based ablation. First, we optimized microglia ablation in mice with normal *Vldlr* expression. *Tmem119*<sup>CreER/+</sup>*Rosa*<sup>DTR/+</sup> mice were given 9 injections of tamoxifen from 3 to 6 weeks of age followed by 4 daily injections of PBS or DT (Fig S3A). Retinal flatmounts were imaged at the level

of the deep capillary plexus where only retinal microglia reside [30]. DT treatment decreased retinal microglia density by 33% compared to PBS control ( $p < 0.01$ , Fig S2B-D). Next, *Vldlr*<sup>-/-</sup>*Tmem119*<sup>CreER/+</sup>*Rosa*<sup>DTR/+</sup> mice were generated, treated with 9 tamoxifen injections from 3 to 6 weeks of age, given 4 daily injections of PBS or DT, and sacrificed on Day 5 (post-DT treatment) for choroidal wholemount imaging (Fig. 4A). Choroidal wholemounts staining for DTR in PBS-treated mice showed that this strategy led to DTR expression in 48% of macrophages at CNV lesions, targeting them for depletion (Fig S3F-H). These data suggest that half of macrophages in CNV lesions are microglia and could be ablated by DT

treatment. Only half of macrophages at CNV lesions expressed DTR either because the *Tmem119*<sup>CreER</sup>-based targeting was inefficient, or because this population includes other macrophages subtypes like choroidal macrophages. Representative images of PBS- and DT-treated *Vldlr*<sup>-/-</sup>*Tmem119*<sup>CreER/+</sup>*Rosa*<sup>DTR/+</sup> mice are shown in Fig. 4B-C. DT treatment reduced macrophage counts in CNV lesions by 21% ( $p < 0.05$ , Fig. 4D), CNV lesion number by 16% ( $p < 0.05$ , Fig. 4E), but did not affect total CNV lesion area (Fig. 4F). Data split by sex can be found in Fig S4, which showed slightly greater effects in females than males but overall similar trends. The greater effect in females correlated with improved macrophage depletion

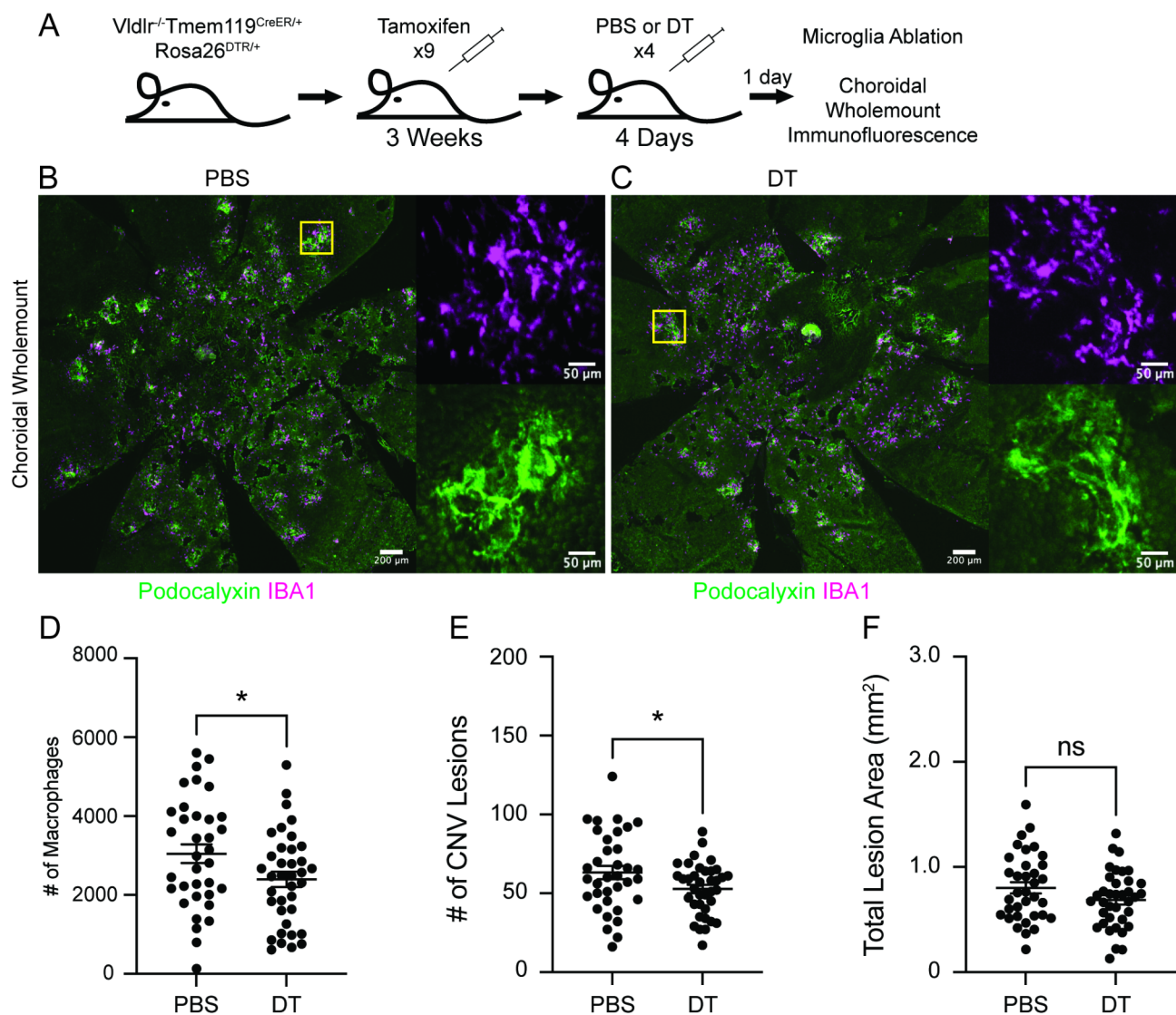


**Fig. 4** Microglia depletion slightly decreases CNV number in *Vldlr*<sup>-/-</sup>*Tmem119*<sup>CreER/+</sup>*Rosa*<sup>DTR/+</sup> mice. **A:** Schematic for injection strategy in *Vldlr*<sup>-/-</sup>*Tmem119*<sup>CreER/+</sup>*Rosa*<sup>DTR/+</sup> mice. **B-C:** Representative choroidal wholemount images of PBS- and DT-treated *Vldlr*<sup>-/-</sup>*Tmem119*<sup>CreER/+</sup>*Rosa*<sup>DTR/+</sup> mice stained for IBA1 (macrophages) and Podocalyxin (choriocapillaris). Insets are outlined in yellow. DT (diphtheria toxin) treatment reduced macrophage counts (**D**, Student's unpaired t-test) and decreased the number of CNV lesions (**E**, Welch's t-test). DT treatment but had no effect upon total CNV lesion area (**F**, Student's unpaired t-test). \*  $p < 0.05$ , ns = not significant.  $N = 35-37$  mice per group



at CNV lesions. These data suggest that microglia may have a limited role in spontaneous CNV in the *Vldlr*<sup>-/-</sup> model. However, microglia ablation by 33% was not optimal and so we sought to ablate microglia via a complementary strategy.

We generated *Cx3cr1*<sup>CreER</sup>*Csf1r*<sup>iDTR</sup> mice, which non-selectively target all macrophages [33]. In this model, tamoxifen treatment will induce CRE expression in monocytes and macrophages. Next, CRE will remove the stop codon from cells also expressing *Csf1r*, leading to DTR expression and susceptibility to DT-based ablation. *Cx3cr1*<sup>CreER</sup> is highly expressed in microglia and a single tamoxifen treatment will target >95% of cells in prior studies using reporter mice [17]. In the choroid, however, a single tamoxifen treatment only targets ~30% of choroidal macrophages in prior studies [17]. Since choroidal macrophages are derived from blood monocytes [17], we treated 4-week-old *Cx3cr1*<sup>CreER</sup>*Csf1r*<sup>iDTR</sup> mice with a single low dose tamoxifen injection and allowed for a 2-week wash out period before PBS or DT administration. Thus, a single tamoxifen dose will target microglia efficiently and ~30% of choroidal macrophages [17]. The 2-week washout period will allow some choroidal macrophage re-population from blood monocytes so that microglia will be more selectively depleted by PBS or DT treatment (Fig S5A). This strategy significantly reduced retinal microglia in the deep capillary plexus by 46% ( $p < 0.01$ , Fig S5B-D) while macrophage density in the choroid was not significantly changed (Fig S5E-G). This strategy demonstrated improved microglia targeting without significantly affecting choroidal macrophages. *Vldlr*<sup>-/-</sup>*Cx3cr1*<sup>CreER</sup>*Csf1r*<sup>iDTR</sup> mice were treated identically with a single low-dose tamoxifen at Week 4 followed by daily PBS or DT injections for 4 days two weeks post-tamoxifen (Fig. 5A). DT treatment decreased macrophage counts at CNV lesions by 51% ( $p < 0.0001$ , Fig. 5B-D), reduced lesion number by 18% ( $p < 0.05$ , Fig. 5E), but did not affect total CNV lesion area (Fig. 5F). Data split by sex can be found in Fig S6, which showed greater effects in females than males but overall similar trends. The larger effect in females correlated with more macrophage depletion at CNV lesions. This complementary approach affirms that microglia may serve a role in CNV lesion initiation as suggested by lower lesion numbers, but may not affect lesion growth and/or maintenance since total lesion area was unaffected.

To investigate the role of choroidal macrophages, we treated *Cx3cr1*<sup>CreER</sup>*Csf1r*<sup>iDTR</sup> mice with 9 tamoxifen injections over 3–6 weeks of age to both target microglia and recycling choroidal macrophages (Fig S7A). Since *Cx3cr1*<sup>CreER</sup> is highly expressed in microglia, 9 tamoxifen injections will very efficiently target microglia. Since tamoxifen treatment in *Cx3cr1*<sup>CreER</sup> mice targets ~30% of choroidal macrophages, choroidal macrophages are

derived from blood monocytes [17], and tamoxifen treatment targets ~70% of blood monocytes [25], 9 tamoxifen injections over 3 weeks should target existing choroidal macrophages by at least 30% and choroidal macrophages repopulated from blood monocytes. Daily PBS or DT treatment for 4 days, after 9 tamoxifen injections over 3 weeks, decreased retinal microglia by 99% ( $p < 0.0001$ , Fig S7B-D) and choroidal macrophages by 95% ( $p < 0.0001$ , Fig S7E-G). These data suggest that our strategy effectively targets both retinal microglia and choroidal macrophages. *Vldlr*<sup>-/-</sup>*Cx3cr1*<sup>CreER</sup>*Csf1r*<sup>iDTR</sup> mice were similarly treated with 9 tamoxifen injections from 3 to 6 weeks of age followed by 4 daily PBS or DT treatments (Fig. 6A). DT treatment decreased macrophages numbers at CNV lesions by 87% ( $p < 0.0001$ , Fig. 6B-D), lesion number by 59% ( $p < 0.0001$ , Fig. 6E), and total lesion area by 73% ( $p < 0.0001$ , Fig. 6F). Data split by sex can be found in Fig S8. These data suggest that the ablation of retinal microglia and choroidal macrophages impacts spontaneous CNV initiation and propagation. In the context of the results from microglia targeting studies (Figs. 4 and 5), choroidal macrophages may be the key macrophages for CNV growth in the *Vldlr*<sup>-/-</sup> mouse.

## Discussion

Myeloid cells are potential therapeutic targets for anti-VEGF treatment resistant patients with neovascular AMD. While the role of myeloid cells and their heterogeneity in the laser-induced CNV model is well known, the role of myeloid cells in the *Vldlr*<sup>-/-</sup> spontaneous CNV model is less well established. By breeding the *Vldlr*<sup>-/-</sup> mouse into the *Ccr2*<sup>-/-</sup> and *Nr4a1*<sup>-/-</sup> backgrounds, we found that both classical and non-classical monocytes and their monocyte-derived macrophages are dispensable for CNV in *Vldlr*<sup>-/-</sup> mice (Figs. 2 and 3). We next generated two separate microglia targeting strategies that yielded the same results: microglia depletion reduces CNV numbers but not CNV area (Figs. 4 and 5). Finally, we ablated both choroidal macrophages and microglia with high efficiency and found that CNV number and area were severely decreased (Fig. 6). Taken together, our results suggest that microglia are potential CNV initiators while choroidal macrophages are the likely most important macrophages for CNV growth and maintenance.

Our results expand and agree with key prior work. Usui-Ouchi et al. previously showed that microglia migrate from the outer plexiform layer into the subretinal space at Week 2 in *Vldlr*<sup>-/-</sup> mice [8]. Additionally, depletion of posterior segment macrophages— including microglia and choroidal macrophages— with CSF1R antagonist (Fig S1), decreases CNV number [8], but CNV area was not calculated. Further, genetic macrophage targeting with *Cx3cr1*<sup>CreER</sup>*Rosa26*<sup>DTR</sup> mice receiving

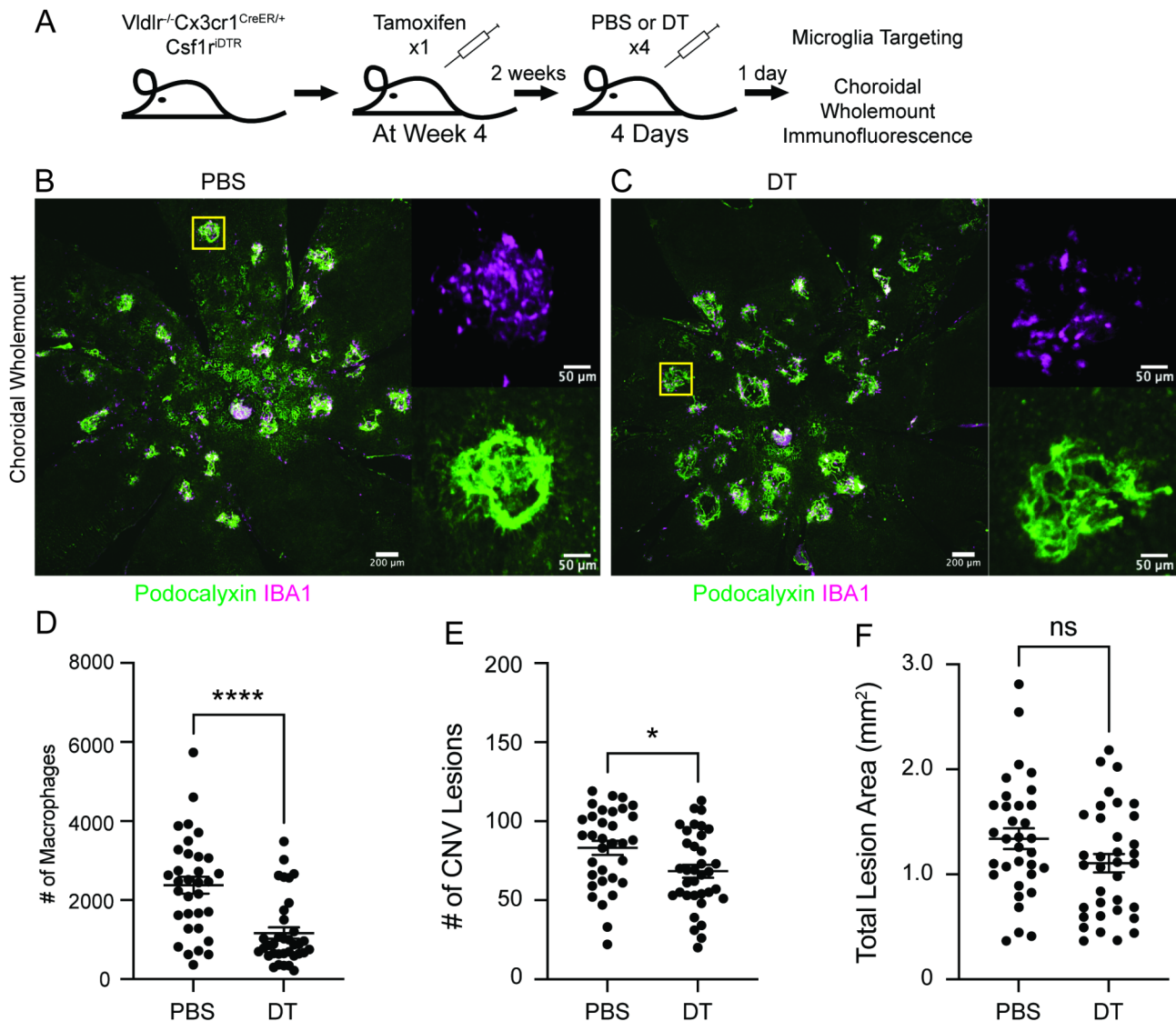


**Fig. 5** Microglia reduction decreases CNV number in  $Vldlr^{-/-}Cx3cr1^{CreER}/Csf1^{rDTR}$  mice. **A:** Schematic for injection strategy in  $Vldlr^{-/-}Cx3cr1^{CreER}/Csf1^{rDTR}$  mice. **B–C:** Representative choroidal wholemount images of PBS- and DT-treated  $Vldlr^{-/-}Cx3cr1^{CreER}/Csf1^{rDTR}$  mice stained for IBA1 (macrophages) and Podocalyxin (choriocapillaris). Insets are outlined in yellow. DT (diphtheria toxin) treatment reduced macrophage counts (**D**, Mann-Whitney test) and decreased the number of CNV lesions (**E**, Student's unpaired t-test). DT treatment but had no effect upon total CNV lesion area (**F**, Student's unpaired t-test). \*\*\*\*  $p < 0.0001$ , \*  $p < 0.05$ , ns = not significant.  $N = 33$ – $35$  mice per group

tamoxifen at P10 and P11 followed by DT treatment from P12–P14 decreases CNV lesion number [8], but CNV area was not calculated. We did not test this exact regimen of tamoxifen without washout, but we suspect from our studies that microglia would be well depleted while some choroidal macrophage depletion would also occur. In agreement, 48 h post two tamoxifen treatments, choroidal macrophages are  $\sim 30\%$  GFP<sup>+</sup> in  $Cx3cr1^{CreER}/Rosa26^{GFP}$  mice [17]. Therefore, prior work by Usui-Ouchi et al. in  $Vldlr^{-/-}$  mice [8], shows that CNV number is reduced by targeting both microglia and choroidal macrophages to an unknown extent. Our work expands upon these results by investigating microglia independently.

In two microglia-specific targeting strategies, microglia depletion by 33% (Fig S2) leads to a 16% reduction in CNV number (Fig. 4). Similarly, microglia depletion by 46% (Fig S3) results in a 18% reduction in CNV number (Fig. 5). These results may demonstrate that a dose-dependent reduction in microglia reduces CNV number. Since microglia migrate into the subretinal space at Week 2 with pathological endothelial cells [8], our results suggest that microglia are important for the initiation of CNV. These results also agree with the initiation process, which includes hypoxia-induced factor 1 stabilization and increased VEGF production by photoreceptors [7],

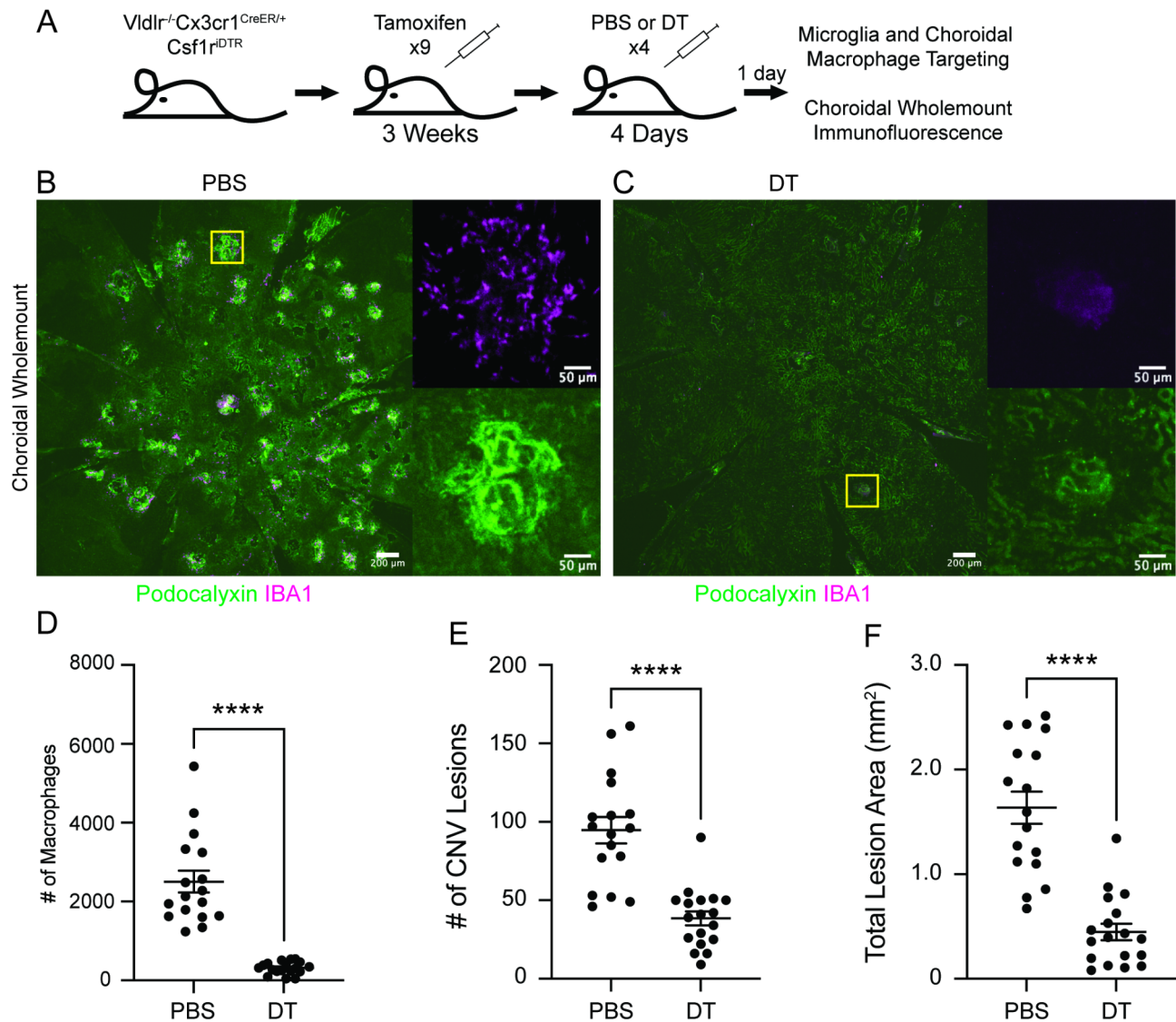


**Fig. 6** Microglia and choroidal macrophage ablation severely impacts CNV number and lesion area in *Vldlr*<sup>-/-</sup>*Cx3cr1*<sup>CreER</sup>*Csf1r*<sup>DTR</sup> mice. **A:** Schematic for injection strategy in *Vldlr*<sup>-/-</sup>*Cx3cr1*<sup>CreER</sup>*Csf1r*<sup>DTR</sup> mice. **B–C:** Representative choroidal wholemount images of PBS- and DT-treated *Vldlr*<sup>-/-</sup>*Cx3cr1*<sup>CreER</sup>*Csf1r*<sup>DTR</sup> mice stained for IBA1 (macrophages) and Podocalyxin (choriocapillaris). Insets are outlined in yellow. DT (diphtheria toxin) treatment reduced macrophage counts (**D**, Mann-Whitney test), decreased the number of CNV lesions (**E**, Welch's t-test), and lessened total CNV lesion area (**F**, Mann-Whitney test). \*\*\*\*  $p < 0.0001$ .  $N = 17$ – $18$  mice per group

which occur on the retinal side of an intact blood-ocular barrier early in the CNV process.

Since microglia reduction alone did not reduce CNV lesion area (Figs. 4 and 5) but choroidal macrophage and microglia ablation severely decreased CNV lesion area (Fig. 6), our data suggest that choroidal macrophages are necessary for CNV lesion growth and/or maintenance. To ablate choroidal macrophages, we used 9 tamoxifen injections, which led to a 99% reduction in microglia with a 95% decrease in choroidal macrophages. One could theorize whether severe microglia depletion resulted in the absence of CNV initiation, thus severely depleting CNV area. However, our depletion was done at 6 weeks

of age, after a large amount of CNV initiation had already occurred. Therefore, severe macrophage depletion led to both CNV regression in terms of lesion size and number. The mechanism by which this occurs is unknown; possible explanations include paracrine factors that stimulate angiogenesis, prevention of endothelial cell apoptosis via paracrine or other mechanisms, or maintenance of RPE health. Interestingly, choroidal macrophage ablation leads to choriocapillaris and RPE atrophy [34]. Since choroidal macrophage ablation causes a reduction in VEGF levels [34] and RPE-specific ablation of *Vegfa* decreases CNV number in *Vldlr*<sup>-/-</sup> mice [8], choroidal macrophage maintenance of RPE health and VEGF production is a



possible mechanism by which choroidal macrophages maintain CNV in *Vldlr*<sup>-/-</sup> mice. This mechanism is potentially supported by transcriptional profiling with bulk RNA-seq of resident macrophages in *Vldlr*<sup>-/-</sup> mice, which showed that among all pro-angiogenic genes only *Angptl7*, *Serpinf1*, and *Ccl12* were increased [32]. Furthermore, inhibition of CCL12 had no effect upon CNV size or area in *Vldlr*<sup>-/-</sup> mice [32]. Therefore, our working hypothesis is that choroidal macrophages prevent endothelial cell apoptosis and maintain CNV in *Vldlr*<sup>-/-</sup> mice. In the absence of choroidal macrophages, CNV lesions regress due to loss of RPE-driven VEGF production and/or direct choriocapillaris cell death via an unknown mechanism. Future studies will investigate the mechanism by which choroidal macrophages maintain CNV.

We were very surprised to find that classical monocyte deficiency, using *Ccr2*<sup>-/-</sup> mice, had no effect upon CNV macrophage counts nor CNV number or area in *Vldlr*<sup>-/-</sup> mice (Fig. 2). Alternatively, our group and others have shown that laser-induced CNV area is reduced in classical monocyte-deficient *Ccr2*<sup>-/-</sup> mice [25, 26, 27]. Why the discrepancy between laser-induced CNV area and *Vldlr*<sup>-/-</sup> mice? We suspect that the difference results from the lack of acute inflammation in *Vldlr*<sup>-/-</sup> mice compared to the laser-induced CNV model, which is highly inflammatory. Could classical monocytes still be important despite the lack of CCR2 signaling? It is possible, but we feel that this is unlikely because *Ccr2*<sup>-/-</sup> mice also have deficient classical monocyte numbers as well as function [28]. This hypothesis is confirmed by prior studies, which showed that monocytes are not present in CNV lesions in *Vldlr*<sup>-/-</sup> mice [32].

All the studies on *Vldlr*<sup>-/-</sup> mice were performed at 6 weeks of age. Compared to the literature, our studies at 6 weeks are older than the other seminal myeloid cell study at 2–4 weeks of age [8]. This decision was primarily pragmatic. The *Tmem119*<sup>CreER</sup> is unfortunately inefficient, requiring multiple injections and high tamoxifen doses to target retinal microglia both in our hands and in the literature [22]. To prevent high rates of mouse death, we waited until 3 weeks of age to begin tamoxifen injections and performed 9 injections over 3 weeks to target 50% and deplete only 33% of retinal microglia. Because this study was so crucial to our results, we matched all other studies with this age for comparison between results. Although 6-week-old mice are not fully mature, the key results of our studies agree with prior work [8] that depleting all ocular myeloid cells either with CSF1R antagonism or *Cx3cr1*<sup>CreER</sup> mediated DT-based ablation reduced macrophages at CNV lesions, CNV number, and CNV area. Nevertheless, repeating these key studies in fully mature 3–4 month old mice may be prudent.

It is worth noting that CSF1R antagonism and 9 tamoxifen injections followed by DT-based ablation in

*Vldlr*<sup>-/-</sup> *Cx3cr1*<sup>CreER</sup> *Csf1r*<sup>iDTR</sup> mice demonstrated identical and dose-dependent results (Figs. 1 and 6). CSF1R inhibition decreased macrophages at CNV lesions by 63% and CNV area by 48% (Fig. 1). DT treatment in *Vldlr*<sup>-/-</sup> *Cx3cr1*<sup>CreER</sup> *Csf1r*<sup>iDTR</sup> mice reduced macrophages at CNV lesions by 87% and CNV area by 73% (Fig. 6). The fact that greater macrophage depletion at CNV lesions resulted in greater CNV area reduction strengthens the importance of macrophages to this process and provides rigor and reproducibility. Further, each strategy to deplete macrophages has strengths and weaknesses. CSF1R antagonism is a receptor tyrosine kinase inhibitor that inhibits CSF1R with IC<sub>50</sub> of 2 nM, but also inhibits VEGF receptor 2 (VEGFR2, IC<sub>50</sub> = 12 nM). Thus, the effects of CSF1R antagonism could be related to VEGFR2 inhibition instead of macrophage depletion. Alternatively, 9 tamoxifen injections followed by 4 DT treatment also potentially has off target effects. The tamoxifen injections inhibit estrogen (although the effects were similar in male and female mice) and DT-based ablation will affect macrophages in other tissues. Although each strategy has strengths and weaknesses, it is reassuring that the results phenocopy one another.

This study has several limitations. First, our attempts to ablate microglia were not as efficient as desired. We were able to specifically target microglia with 33–46% depletions. It would have been ideal to target 100% of microglia with *Tmem119*<sup>CreER</sup> mice; however, despite 9 intraperitoneal tamoxifen injections at 200 mg/kg and high dose DT at 500 ng, this was not achievable. Second, despite using a state-of-the-art model like *Tmem119*<sup>CreER</sup> mice, because our tamoxifen use was done over a long duration to increase ablation effectiveness, it is unknown if choroidal macrophages could migrate into the subretinal space and upregulate *Tmem119* expression, resulting in a mixed lineage ablation. Third, due to our poor understanding of choroidal macrophages, no models exist to specifically target choroidal macrophages and not microglia. Therefore, our choroidal macrophage ablating mice are hampered by simultaneous microglia ablation. However, by comparing the results of microglia ablation versus microglia and choroidal macrophage ablation, conclusions can be drawn regarding the potential role of choroidal macrophages. Finally, DT-based ablation may have unknown off target effects. However, since CSF1R antagonism to deplete myeloid cells and DT-based myeloid cell depletion showed identical effects on CNV, it is unlikely that the phenotype is a result of off target actions.

## Conclusions

In summary, we found that monocytes and monocyte-derived macrophages are dispensable for CNV in *Vldlr*<sup>-/-</sup> mice. Microglia depletion decreased CNV number and



likely affects CNV initiation. Choroidal macrophage and microglia ablation severely reduces CNV number and total area, suggesting that choroidal macrophages are potentially crucial for CNV growth and/or maintenance. Future studies will aim to ablate choroidal macrophages independent of microglia and investigate the mechanism by which choroidal macrophages maintain CNV.

#### Abbreviations

AMD	Age related macular degeneration
CNV	Choroidal neovascularization
VEGF	Vascular endothelial growth factor
VLDLR	Very-low-density lipoprotein receptor
CSF1R	Colony stimulating factor 1 receptor
DT	Diphtheria toxin
DTR	Diphtheria toxin receptor
RPE	Retinal pigment epithelium
VEGF	Vascular endothelial growth factor receptor 2

## Supplementary Information

The online version contains supplementary material available at <https://doi.org/10.1186/s12974-025-03398-3>.

Supplementary Material 1: **Fig. S1. Title of Data** Colony stimulating factor 1 receptor (CSF1R) blockade reduces CNV area split by sex. **Description of Data:** Data for number of CNV lesions, CNV area, and IBA1+ cells at lesions split by sex from Fig. 1.

Supplementary Material 2: **Fig. S2. Title of Data** Colony stimulating factor 1 receptor (CSF1R) blockade reduces microglia and choroidal macrophage density. **Description of Data** A: Schematic for injection strategy. B-C: Representative retinal wholemount images of DMSO vehicle control and CSF1R inhibitor (INH) treated mice stained for IBA1 (macrophages) and CD31 (endothelial cells). CSF1R inhibition reduced retinal microglia density (D, Student's un-paired t-test). E-F: Representative bleached choroidal wholemount images of DMSO vehicle control and CSF1R inhibitor (INH) treated mice stained for IBA1 (macrophages) and Podocalyxin (choriocapillaris). CSF1R inhibition reduced choroidal macrophage density (G, Student's un-paired t-test). \*\*\*\*  $p < 0.0001$ .  $N = 6$  mice per group.

Supplementary Material 3: **Fig. S3. Title of Data** Microglia depletion in *Tmem119<sup>CreER/+</sup>Rosa<sup>DTR/+</sup>* mice. **Description of Data:** A: Schematic for injection strategy in *Tmem119<sup>CreER/+</sup>Rosa<sup>DTR/+</sup>* mice. B-C: Representative retinal wholemount images of PBS- and DT-treated *Tmem119<sup>CreER/+</sup>Rosa<sup>DTR/+</sup>* mice stained for IBA1 (macrophages) and CD31 (endothelial cells). DT (diphtheria toxin) treatment reduced microglia density (D, Student's unpaired t-test,  $N = 5-7$  mice per group) E: Schematic for injection strategy in *Vldlr<sup>-/-</sup>Tmem119<sup>CreER/+</sup>Rosa<sup>DTR/+</sup>* mice. F-G: Representative choroidal wholemount images of PBS-treated *Vldlr<sup>-/-</sup>Tmem119<sup>CreER/+</sup>Rosa<sup>DTR/+</sup>* mice stained for IBA1 (macrophages), CD31 (endothelial cells), and DTR. H: 48% of IBA1+ macrophages were also DTR+ ( $N = 6$  mice). \*\*  $p < 0.01$ .

Supplementary Material 4: **Fig. S4. Title of data** Microglia depletion slightly decreases CNV number in *Vldlr<sup>-/-</sup>Tmem119<sup>CreER/+</sup>Rosa<sup>DTR/+</sup>* mice. **Description of data** Data for number of CNV lesions, CNV area, and IBA1+ cells at lesions split by sex from Fig. 4.

Supplementary Material 5: **Fig. S5. Title of data** *Cx3cr1<sup>CreER</sup>Csf1r<sup>DTR</sup>* mice can target microglia. **Description of Data:** A: Schematic for injection strategy in *Cx3cr1<sup>CreER</sup>Csf1r<sup>DTR</sup>* mice. B-C: Representative retinal wholemount images of PBS- and DT-treated *Cx3cr1<sup>CreER</sup>Csf1r<sup>DTR</sup>* mice stained for IBA1 (macrophages) and CD31 (endothelial cells). D: DT (diphtheria toxin) treatment reduced microglia density (Welch's t-test,  $N = 7$  mice per group). E-F: Representative bleached choroidal wholemount images of PBS- and DT-treated *Cx3cr1<sup>CreER</sup>Csf1r<sup>DTR</sup>* mice stained for IBA1 (macrophages) and Podocalyxin (choriocapillaris). G: DT treatment but had no significant effect upon choroidal macrophage density (Welch's t-test,  $N = 7$  mice per group). \*\*  $p < 0.01$ , ns = not significant.

Supplementary Material 6: **Fig. S6. Title of data** Microglia reduction decreases CNV number in *Vldlr<sup>-/-</sup>Cx3cr1<sup>CreER</sup>Csf1r<sup>DTR</sup>* mice. **Description of data** Data for number of CNV lesions, CNV area, and IBA1+ cells at lesions split by sex from Fig. 5.

Supplementary Material 7: **Fig. S7. Title of data** *Cx3cr1<sup>CreER</sup>Csf1r<sup>DTR</sup>* mice can target choroidal macrophages and microglia with additional tamoxifen treatment. **Description of Data:** A: Schematic for injection strategy in *Cx3cr1<sup>CreER</sup>Csf1r<sup>DTR</sup>* mice. B-C: Representative retinal wholemount images of PBS- and DT-treated *Cx3cr1<sup>CreER</sup>Csf1r<sup>DTR</sup>* mice stained for IBA1 (macrophages) and CD31 (endothelial cells). D: DT (diphtheria toxin) treatment significantly reduced microglia density (Welch's t-test,  $N = 7-8$  mice per group). E-F: Representative bleached choroidal wholemount images of PBS- and DT-treated *Cx3cr1<sup>CreER</sup>Csf1r<sup>DTR</sup>* mice stained for IBA1 (macrophages) and Podocalyxin (choriocapillaris). G: DT treatment significantly decreased choroidal macrophage density (Welch's t-test,  $N = 7-8$  mice per group). \*\*\*\*  $p < 0.0001$ .

Supplementary Material 8: **Fig. S8. Title of data** Microglia and choroidal macrophage ablation severely impacts CNV number and lesion area in *Vldlr<sup>-/-</sup>Cx3cr1<sup>CreER</sup>Csf1r<sup>DTR</sup>* mice. **Description of data** Data for number of CNV lesions, CNV area, and IBA1+ cells at lesions split by sex from Fig. 6.

Supplementary Material 9: **Table S1. Title of Data** Antibodies. **Description of Data:** Antibodies and dilutions used. **Title of Data** Raw Graph Data. **Description of Data:** Raw data of all graphs

#### Acknowledgements

None.

#### Author contributions

AR's role was investigation, formal analysis, methodology, and writing the original draft. JG, RV, KSC, and SD performed investigation, formal analysis, methodology, and writing review and editing. DK, JS, and ALW performed investigation, formal analysis, and writing review and editing. JAL's roles were conceptualization, data curation, formal analysis, funding acquisition, investigation, methodology, project administration, supervision, visualization, and writing the original draft as well as editing and review.

#### Funding

This study was supported by a BrightFocus New Investigator Award and an Unrestricted Departmental Grant from Research to Prevent Blindness. JAL was supported by NIH grant K08 EY030923, R01 EY034486, and the Research to Prevent Blindness Sybil B. Harrington Career Development Award for Macular Degeneration. KSC was supported by the Research to Prevent Blindness Medical Student Eye Research Fellowship. Imaging work was performed at the Northwestern University Center for Advanced Microscopy generously supported by CCSG P30 CA060553 awarded to the Robert H Lurie Comprehensive Cancer Center. No funding body had any role in the design of the study, collection, analysis, interpretation of data, or in writing the manuscript. JAL is a consultant for Line 6 Biotechnology and Genentech. JAL received research grant support from Therini Bio. No company body had any role in the design of the study, collection, analysis, interpretation of data, or in writing the manuscript. The authors have no additional financial interests.

#### Data availability

All data will be available upon reasonable request to the corresponding author. All data values in graphs are available in the supporting data values (Raw Graph Data) excel sheet.

#### Declarations

#### Study approval

All studies were performed in accordance with protocols approved by the Northwestern University Institutional Animal Care and Use Committee.

#### Consent for publication

Not applicable.

## Competing interests

JAL is a consultant for Line 6 Biotechnology and Genentech. JAL received research grant support from Therini Bio. No company body had any role in the design of the study, collection, analysis, interpretation of data, or in writing the manuscript. The authors have no additional financial interests.

Received: 2 January 2025 / Accepted: 24 February 2025

Published online: 07 March 2025

## References

1. Danis RP, Lavine JA, Domalpally A. Geographic atrophy in patients with advanced dry age-related macular degeneration: current challenges and future prospects. *Clin Ophthalmol* (Auckl NZ). 2015;9:2159–74.
2. Lim LS, Mitchell P, Seddon JM, Holz FG, Wong TY. Age-related macular degeneration. *The Lancet* [Internet]. 2012;379:1728–38. Available from: [https://doi.org/10.1016/S0140-6736\(12\)60282-7](https://doi.org/10.1016/S0140-6736(12)60282-7)
3. Group CR, Martin DF, Maguire MG, Ying G, Grunwald JE, Fine SL et al. Ranibizumab and Bevacizumab for Neovascular Age-Related Macular Degeneration. *New Engl J Medicine* [Internet]. 2011;364:1897–908. Available from: <http://eutils.ncbi.nlm.nih.gov/entrez/eutils/elink.fcgi?dbfrom=pubmed%26;id=21526923%26;retmode=ref%26;cmd=prlinks>
4. Heier JS, Khanani AM, Ruiz CQ, Basu K, Ferrone PJ, Brittain C et al. Efficacy, durability, and safety of intravitreal faricimab up to every 16 weeks for neovascular age-related macular degeneration (TENAYA and LUCERNE): two randomised, double-masked, phase 3, non-inferiority trials. *Lancet* [Internet]. 2022;399:729–40. Available from: [https://doi.org/10.1016/S0140-6736\(22\)00010-1](https://doi.org/10.1016/S0140-6736(22)00010-1)
5. Lanzetta P, Korobelnik J-F, Heier JS, Leal S, Holz FG, Clark WL, et al. Intravitreal Aflibercept 8 mg in neovascular age-related macular degeneration (PULSAR): 48-week results from a randomised, double-masked, non-inferiority, phase 3 trial. *Lancet*. 2024;403:1141–52.
6. HECKENLIVELY JR, HAWES NL, FRIEDLANDER M, NUSINOWITZ S, HURD R, DAVISSON M, et al. MOUSE MODEL OF SUBRETINAL NEOVASCULARIZATION WITH CHOROIDAL ANASTOMOSIS. *RETINA*. 2003;23:518–22.
7. Joyal J-S, Sun Y, Gantner ML, Shao Z, Evans LP, Saba N, et al. Retinal lipid and glucose metabolism dictates angiogenesis through the lipid sensor Ffar1. *Nat Med*. 2016;22:439–45.
8. Usui-Ouchi A, Usui Y, Kurihara T, Aguilar E, Dorrell MI, Ideguchi Y et al. Retinal microglia are critical for subretinal neovascular formation. *JCI Insight* [Internet]. 2020;5:1149–14. Available from: <https://insight.jci.org/articles/view/137317>
9. Edwards AO, Ritter R, Abel KJ, Manning A, Panhuysen C, Farrer LA. Complement factor H polymorphism and age-related macular degeneration. *Science* [Internet]. 2005;308:421–4. Available from: <http://www.sciencemag.org/content/308/5720/421.short>
10. Klein RJ, Zeiss C, Chew EY, Tsai J-Y, Sackler RS, Haynes C et al. Complement factor H polymorphism in age-related macular degeneration. *Science* [Internet]. 2005;308:385–9. Available from: <http://eutils.ncbi.nlm.nih.gov/entrez/eutils/elink.fcgi?dbfrom=pubmed%26;id=15761122%26;retmode=ref%26;cmd=prlinks>
11. Gold B, Merriam JE, Zernant J, Hancox LS, Taiber AJ, Gehrs K et al. Variation in factor B (BF) and complement component 2 (C2) genes is associated with age-related macular degeneration. *Nat Genet* [Internet]. 2006;38:458–62. Available from: <http://www.nature.com/doi/10.1038/ng1750>
12. Yates JRW, Sepp T, Matharu BK, Khan JC, Thurlby DA, Shahid H et al. Complement C3 Variant and the Risk of Age-Related Macular Degeneration. *N Engl J Med* [Internet]. 2007;357:553–61. Available from: <http://www.nejm.org/doi/abs/https://doi.org/10.1056/NEJMoa072618>
13. Grossniklaus HE, Martinez JA, Brown VB, Lambert HM, Sternberg P, Capone A et al. Immunohistochemical and histochemical properties of surgically excised subretinal neovascular membranes in age-related macular degeneration. *American Journal of Ophthalmology* [Internet]. 1992;114:464–72. Available from: <http://eutils.ncbi.nlm.nih.gov/entrez/eutils/elink.fcgi?dbfrom=pubmed%26;id=1415458%26;retmode=ref%26;cmd=prlinks>
14. Lopez PF, Grossniklaus HE, Lambert HM, Aaberg TM, Capone A, Sternberg P et al. Pathologic features of surgically excised subretinal neovascular membranes in age-related macular degeneration. *American Journal of Ophthalmology* [Internet]. 1991;112:647–56. Available from: <http://eutils.ncbi.nlm.nih.gov/entrez/eutils/elink.fcgi?dbfrom=pubmed%26;id=1957899%26;retmode=ref%26;cmd=prlinks>
15. Espinosa-Heidmann DG, Suner IJ, Hernandez EP, Monroy D, Csaky KG, Cousins SW. Macrophage depletion diminishes lesion size and severity in experimental choroidal neovascularization. *Invest Ophthalmology Vis Sci*. 2003;44:3586.
16. Sakurai E, Anand A, Ambati BK, van Rooijen N, Ambati J. Macrophage depletion inhibits experimental choroidal neovascularization. *Investigative Ophthalmology & Visual Science* [Internet]. 2003;44:3578–85. Available from: <http://eutils.ncbi.nlm.nih.gov/entrez/eutils/elink.fcgi?dbfrom=pubmed%26;id=12882810%26;retmode=ref%26;cmd=prlinks>
17. O'Koren EG, Yu C, Klingeborn M, Wong AYW, Prigge CL, Mathew R et al. Microglial Function Is Distinct in Different Anatomical Locations during Retinal Homeostasis and Degeneration. *Immunity* [Internet]. 2019;1–23. Available from: <https://doi.org/10.1016/j.immuni.2019.02.007>
18. O'Koren EG, Mathew R, Saban DR. Fate mapping reveals that microglia and recruited monocyte-derived macrophages are definitively distinguishable by phenotype in the retina. *Nature Publishing Group* [Internet]. 2016;1–12. Available from: <https://doi.org/10.1038/srep20636>
19. Ruan C, Sun L, Kroshilina A, Beckers L, Jager PD, Bradshaw EM, A novel Tmem119-tdTomato reporter mouse model for studying microglia in the central nervous system. *Brain et al. Behavior, and Immunity* [Internet]. 2020;83:180–91. Available from: <https://doi.org/10.1016/j.bbi.2019.10.009>
20. Kaiser T, Feng G, Tmem. 119-EGFP and Tmem119-CreERT2 Transgenic Mice for Labeling and Manipulating Microglia. *eNeuro* [Internet]. 2019;6:1–18. Available from: <http://eutils.ncbi.nlm.nih.gov/entrez/eutils/elink.fcgi?dbfrom=pubmed%26;id=31371457%26;retmode=ref%26;cmd=prlinks>
21. McKinsey GL, Lizama CO, Keown-Lang AE, Niu A, Santander N, Larphavesarp A et al. A new genetic strategy for targeting microglia in development and disease. *Elife* [Internet]. 2020;9. Available from: <https://elifesciences.org/articles/54590>
22. Bedolla AM, McKinsey GL, Ware K, Santander N, Arnold TD, Luo Y. A comparative evaluation of the strengths and potential caveats of the microglial inducible CreER mouse models. *Cell Rep*. 2024;43:113660.
23. Hanna RN, Carlin LM, Hubbeling HG, Nackiewicz D, Green AM, Punt JA et al. The transcription factor NR4A1 (Nur77) controls bone marrow differentiation and the survival of Ly6C<sup>+</sup> monocytes. *Nat Immunol* [Internet]. 2011;12:778–85. Available from: <http://www.nature.com/articles/ni.2063>
24. Droho S, Voigt AP, Sterling JK, Rajesh A, Chan KS, Cuda CM, et al. NR4A1 deletion promotes pro-angiogenic polarization of macrophages derived from classical monocytes in a mouse model of neovascular age-related macular degeneration. *J Neuroinflammation*. 2023;20:238.
25. Droho S, Thomson BR, Makinde HM, Cuda CM, Perlman H, Lavine JA. Ocular macrophage origin and heterogeneity during steady state and experimental choroidal neovascularization. *Journal of Neuroinflammation* [Internet]. 2020;1–19. Available from: <https://jneuroinflammation.biomedcentral.com/articles/https://doi.org/10.1186/s12974-020-02010-0>
26. Tsutsumi C, Sonoda K-H, Egashira K, Qiao H, Hisatomi T, Nakao S et al. The critical role of ocular-infiltrating macrophages in the development of choroidal neovascularization. *J Leucoc Biol* [Internet]. 2003;74:25–32. Available from: <http://www.jleukbio.org/cgi/doi/https://doi.org/10.1189/jlb.0902436>
27. Tan X, Fujii K, Manabe I, Nishida J, Yamagishi R, Terashima Y et al. Choroidal Neovascularization Is Inhibited in Splenic-Denervated or Splenectomized Mice with a Concomitant Decrease in Intraocular Macrophage. *Abe T, editor. PLoS ONE* [Internet]. 2016;11:e0160985. Available from: <https://doi.org/10.1371/journal.pone.0160985.s003>
28. Boring L, Gosling J, Chensue SW, Kunkel SL, Farese RV, Broxmeyer HE, et al. Impaired monocyte migration and reduced type 1 (Th1) cytokine responses in C-C chemokine receptor 2 knockout mice. *J Clin Invest*. 1997;100:2552–61.
29. Droho S, Rajesh A, Cuda CM, Perlman H, Lavine JA. CD11c<sup>+</sup> macrophages are pro-angiogenic and necessary for experimental choroidal neovascularization. *JCI Insight*. 2023;8:e168142.
30. Sterling JK, Rajesh A, Droho S, Gong J, Wang AL, Voigt AP, et al. Retinal perivascular macrophages regulate immune cell infiltration during neuroinflammation in mouse models of ocular disease. *J Clin Invest*. 2024;134:e180904.
31. Zaitoun IS, Song Y-S, Zaitoun HB, Sorenson CM, Sheibani N. Assessment of choroidal vasculature and innate immune cells in the eyes of albino and pigmented mice. *Cells*. 2022;11:3329.
32. Schlecht A, Wolf J, Boneva S, Prinz G, Braunger BM, Wieghofer P et al. Transcriptional and Distributional Profiling of Microglia in Retinal Angioma-tous Proliferation. *IJMS* [Internet]. 2022;23:3443. Available from: <https://www.mdpi.com/1422-0067/23/7/3443/htm>

33. Yona S, Kim K-W, Wolf Y, Mildner A, Varol D, Breker M et al. Fate Mapping Reveals Origins and Dynamics of Monocytes and Tissue Macrophages under Homeostasis. *Immunity* [Internet]. 2013;38:79–91. Available from: <https://linkinghub.elsevier.com/retrieve/pii/S1074761312005481>
34. Yang X, Zhao L, Campos MM, Abu-Asab M, Ortolan D, Hotaling N et al. CSF1R blockade induces macrophage ablation and results in mouse choroidal vascular atrophy and RPE disorganization. *Elife* [Internet]. 2020;9:18. Available from: <https://elifesciences.org/articles/55564>

### **Publisher's note**

Springer Nature remains neutral with regard to jurisdictional claims in published maps and institutional affiliations.